Stress tensor for a scalar field in a spatially varying background potential: Divergences, "renormalization", anomalies, and Casimir forces

Kimball A. Milton,[1,*] Stephen A. Fulling,[2,†] Prachi Parashar,[3,1,‡] Pushpa Kalauni,[1,§] and Taylor Murphy[1,‖]

[1]*Homer L. Dodge Department of Physics and Astronomy, University of Oklahoma, Norman, Oklahoma 73019-2061, USA*

[2]*Departments of Mathematics and Physics, Texas A&M University, College Station, Texas 77843-3368, USA*

[3]*Department of Physics, Southern Illinois University-Carbondale, Carbondale, Illinois 62091-6899, USA*

(Received 1 February 2016; published 13 April 2016)

Motivated by a desire to understand quantum fluctuation energy densities and stress within a spatially varying dielectric medium, we examine the vacuum expectation value for the stress tensor of a scalar field with arbitrary conformal parameter, in the background of a given potential that depends on only one spatial coordinate. We regulate the expressions by incorporating a temporal-spatial cutoff in the (imaginary) time and transverse-spatial directions. The divergences are captured by the zeroth- and second-order WKB approximations. Then the stress tensor is "renormalized" by omitting the terms that depend on the cutoff. The ambiguities that inevitably arise in this procedure are both duly noted and restricted by imposing certain physical conditions; one result is that the renormalized stress tensor exhibits the expected trace anomaly. The renormalized stress tensor exhibits no pressure anomaly, in that the principle of virtual work is satisfied for motions in a transverse direction. We then consider a potential that defines a wall, a one-dimensional potential that vanishes for $z < 0$ and rises like z^α, $\alpha > 0$, for $z > 0$. Previously, the stress tensor had been computed outside of the wall, whereas now we compute all components of the stress tensor in the interior of the wall. The full finite stress tensor is computed numerically for the two cases where explicit solutions to the differential equation are available, $\alpha = 1$ and 2. The energy density exhibits an inverse linear divergence as the boundary is approached from the inside for a linear potential, and a logarithmic divergence for a quadratic potential. Finally, the interaction between two such walls is computed, and it is shown that the attractive Casimir pressure between the two walls also satisfies the principle of virtual work (i.e., the pressure equals the negative derivative of the energy with respect to the distance between the walls).

DOI: 10.1103/PhysRevD.93.085017

I. INTRODUCTION

When Casimir discovered [1] that, because of quantum fluctuations, two uncharged perfectly conducting parallel plates attracted each other in vacuum, he considered an unphysical abstraction. Lifshitz [2] partially remedied this defect, by allowing the plates to consist of dielectric material with an arbitrary permittivity as a function of frequency, but he still imagined that the plates were separated by vacuum. This omission was removed a few years later with the addition of Dzyaloshinskii and Pitaevskii [3]; now the plates could be separated by another dielectric. But the geometry still was a three-layer system: the dielectric material was spatially constant in each region. The general problem of a spatially varying medium has still not been solved [4]. (Recent papers on this topic include Refs. [5–7].) It is not merely a matter of numerics: Divergences arise associated with this variation that are still not understood. For an overview of the state of knowledge in Casimir physics, see Ref. [8]. In this paper, we use natural units, with $\hbar = c = 1$.

Some years ago, we started a program to investigate such problems in the context of a simpler scalar field interacting with a spatially varying potential. The proposal of a soft wall was made in Ref. [9]; that is, we consider a potential of the form

$$v(z) = \begin{cases} 0, & z < 0, \\ z^\alpha, & z > 0, \end{cases} \tag{1.1}$$

with $\alpha > 0$, the coupling constant being absorbed into the definition of z [9]. This potential interacts with a massless scalar field ϕ governed by the Lagrangian

$$\mathcal{L} = -\frac{1}{2}\partial_\mu\phi\partial^\mu\phi - \frac{v}{2}\phi^2. \tag{1.2}$$

The corresponding stress-energy tensor in flat Minkowski space with $g^{\mu\nu} = \mathrm{diag}(-1, 1, 1, 1)$ is

*milton@nhn.ou.edu
†fulling@math.tamu.edu
‡prachi@nhn.ou.edu
§pushpakalauni60@gmail.com
‖taylormurphy@ou.edu

$$T^{\mu\nu} = \partial^\mu\phi\partial^\nu\phi - \frac{1}{2}g^{\mu\nu}(\partial_\lambda\phi\partial^\lambda\phi + v\phi^2) - \xi(\partial^\mu\partial^\nu - g^{\mu\nu}\partial^2)\phi^2. \tag{1.3}$$

Here, we have included the arbitrary conformal term, with the conformal parameter ξ. The value $\xi = 1/6$ is the one that makes conformal symmetry manifest, and softens many divergences in scalar quantum field theory.

In Ref. [10], we computed the energy density for this model, mostly in the vacuum region below the wall. Once the bulk energy density, which makes no reference to the potential at all, is subtracted, the energy density is finite outside the wall. We showed that the energy density diverges as the boundary is approached from below,

$$z \to 0^-: \; u(z) \sim \frac{1-6\xi}{96\pi^2}\frac{1}{z}, \tag{1.4}$$

for a linear wall, much softer than the $1/z^4$ divergence seen for a Dirichlet wall. For a quadratic wall, the surface divergence is logarithmic,

$$z \to 0^-: \; u(z) \sim -\frac{1-6\xi}{48\pi^2}\Gamma(0, 2|z|). \tag{1.5}$$

For larger values of α, there is no surface divergence at all.

We also analyzed the divergence structure within the walls, where using second-order WKB analysis we showed with a temporal cutoff τ that the energy density had the following dependence:

$$u(z) \sim \frac{3}{2\pi^2}\frac{1}{\tau^4} - \frac{1}{8\pi^2}\frac{v(z)}{\tau^2} + \frac{1}{32\pi^2}\left[v(z)^2 + \frac{2}{3}(1-6\xi)\frac{\partial^2}{\partial z^2}v(z)\right]\ln\tau. \tag{1.6}$$

The first term is the divergent bulk energy density, independent of the potential. The lower-order divergences involve the potential.

The first steps in extending this work have been given in Ref. [11]. There, general formulas are given for all components of the stress tensor, and a strategy for extending the computational ability to general α is sketched. Here we tackle the general problem within the wall, but with detailed numerical results restricted to the explicitly solvable cases $\alpha = 1, 2$.

In Sec. II, we state the general Green's function formulation of the problem, and discuss the point-splitting regulation scheme used to define the vacuum expectation value of the square of the field. We then give formulas for constructing the vacuum expectation value of the stress tensor. In Sec. III, we identify the divergences occurring in the vacuum expectation value of the stress tensor, based on the second-order WKB approximation. In Sec. IV, we give the classically expected trace and divergence equations satisfied by the stress tensor. Since the WKB solutions found in Sec. III are only approximate, the divergence, or conservation, identity is only approximately satisfied in any order of WKB approximation, although the trace identity is automatically satisfied for any g.

The divergences found in Sec. III are systematically discarded in Sec. V. As in the curved-space analogue, at least some of these divergences correspond to terms in the original Lagrangian [9,12,13], so we shall refer to this process as "renormalization." There are logarithmically divergent terms; these transform into finite terms depending logarithmically on the potential with an arbitrary mass scale. The process of renormalizing the stress tensor involves two further steps: the vacuum expectation value of the scalar field is shifted by an amount proportional to the square of the cutoff parameter δ; and the stress tensor is modified by the addition of a term proportional to the second heat-kernel coefficient, so that it does not possess a conservation anomaly. As a consequence, the stress tensor acquires the well known [14] trace anomaly. In this procedure, we follow Wald [15]. The resulting renormalized stress tensor is now diagonal and satisfies the principle of virtual work, displaying no pressure anomaly.

The considerations in Secs. II–V are more general than the steeply rising potential considered in the rest of the paper. They apply to (at least) any positive Klein-Gordon potential that depends on only one Cartesian coordinate.

We then go on in Secs. VI and VII to discuss the energy density in the interior region for the linear and the quadratic potentials, respectively. We compute the finite remainders numerically, and show that they have the expected divergences as the boundary $z = 0$ is approached from above, the same as those found outside (further discussion in Appendix B). The behavior of $\langle T_{zz}\rangle$, which does not exhibit any surface divergence, is discussed in Sec. VIII.

Finally, in Sec. IX, we consider two such walls, with arbitrary, mirrored, potentials. The Lifshitz formula is easily obtained for the force between the walls, which is shown, for arbitrary potential, to be equally well derivable from the total energy obtained by integrating the energy over the regions between as well as inside the potentials. Thus, as expected, the principle of virtual work is once again satisfied.

The Conclusion discusses further directions this work will pursue. It is followed by two Appendixes, the first on the WKB approximation and the second on the derivation of the "surface divergences."

II. GREEN'S FUNCTION AND CONSTRUCTION OF STRESS TENSOR

We will compute in this paper the vacuum expectation value of the stress tensor obtained from the Green's function, which for this $(2+1)$-dimensional spatial geometry has the form

$$G(x,x') = \int \frac{d\omega}{2\pi}\frac{(d\mathbf{k}_\perp)}{(2\pi)^3} e^{-i\omega(t-t')} e^{i\mathbf{k}_\perp\cdot(\mathbf{r}-\mathbf{r}')_\perp} g(z,z';\omega,\mathbf{k}_\perp), \tag{2.1}$$

which satisfies the differential equation,

$$\left(\frac{\partial^2}{\partial t^2} - \nabla^2 + v\right) G(x,x') = \delta(x-x'), \tag{2.2}$$

where x^μ is a four-vector, and so the delta function is a four-dimensional one. The time-ordered product of fields is the quantum correspondent of this Green's function,

$$\langle \mathrm{T}\phi(x)\phi(x')\rangle = \frac{1}{i} G(x,x'). \tag{2.3}$$

It is more than convenient to perform a Euclidean transformation (more than a Wick rotation),

$$\omega \to i\zeta, \qquad (t-t') \to i(\tau-\tau'), \tag{2.4}$$

which is permitted because the Green's function has no singularities in the first and third quadrants. Then the reduced Green's function becomes a function of $\kappa = \sqrt{\zeta^2 + k^2}$, $k = |\mathbf{k}_\perp|$:

$$g(z,z';\omega,\mathbf{k}_\perp) \to g(z,z';\kappa). \tag{2.5}$$

The reduced Green's function then satisfies

$$\left(-\frac{\partial^2}{\partial z^2} + \kappa^2 + v(z)\right) g(z,z') = \delta(z-z'). \tag{2.6}$$

In general, there is no closed form solution to the homogeneous version of this equation; therefore, in the next section, we give the leading and next-to-leading WKB approximations to the solutions of this equation (which capture the asymptotic behavior in any case) and compute the corresponding stress tensor components, obtained by applying a differential operator to Eq. (2.3). These are divergent, so we regulate them by point-splitting in time and transverse space:

$$\tau - \tau' \to \tau \to 0, \qquad (\mathbf{r}-\mathbf{r}')_\perp \to \boldsymbol{\rho} \to 0. \tag{2.7}$$

Everything is expressed in terms of scalar integrals involving δ [11]:

$$\delta = \sqrt{\tau^2 + \rho^2}. \tag{2.8}$$

In particular, the vacuum expectation value of ϕ^2 is given by

$$\langle\phi^2(x)\rangle = \frac{1}{i}\int \frac{d\omega}{2\pi}\frac{(d\mathbf{k}_\perp)}{(2\pi)^2} e^{i\mathbf{k}\cdot\boldsymbol{\delta}} g(z,z;\omega,k) = \frac{1}{2\pi^2}\int_0^\infty d\kappa\kappa^2 g(z,z;\kappa)\frac{\sin\kappa\delta}{\kappa\delta} \equiv I[g(z)]. \tag{2.9}$$

Here, $g(z) = g(z,z)$.

The general expression for the reduced Green's function can be taken as

$$g(z,z') = \frac{1}{w}F(z_>)G(z_<) - \frac{1}{w}F(z)F(z')\frac{G(0) - G'(0)/\kappa}{F(0) - F'(0)/\kappa}, \tag{2.10}$$

where F is a solution of the homogeneous equation,

$$\left(-\frac{\partial^2}{\partial z^2} + \kappa^2 + v(z)\right)\left\{\begin{matrix} F \\ G \end{matrix}\right\} = 0, \tag{2.11}$$

that decays at positive infinity, and w is the Wronskian with a second independent solution G,

$$w = F(z)G'(z) - G(z)F'(z), \tag{2.12}$$

which is independent of z. It is important to note that adding an arbitrary multiple of F to G does not change the Green's function.

All components of the stress tensor can be computed from the Green's function, more particularly in terms of the regulated vacuum expectation value of ϕ^2 (2.9). For example, the energy density is given by [11] ($\beta = \xi - 1/4$),

$$u = \left(\frac{\partial^2}{\partial\tau^2} - \beta\frac{\partial^2}{\partial z^2}\right) I[g(z)], \tag{2.13a}$$

and the xx and yy components of the stress tensor are expressed as

$$\langle T_{xx}\rangle = -\left(\frac{\partial^2}{\partial\rho_x^2} - \beta\frac{\partial^2}{\partial z^2}\right) I[g(z)], \tag{2.13b}$$

and

$$\langle T_{yy}\rangle = -\left(\frac{\partial^2}{\partial\rho_y^2} - \beta\frac{\partial^2}{\partial z^2}\right) I[g(z)], \tag{2.13c}$$

while the zz component is written as

$$\langle T_{zz}\rangle = \frac{1}{4}\frac{\partial^2}{\partial z^2} I[g(z)] - I[(\kappa^2 + v(z))g(z)]. \tag{2.13d}$$

The off-diagonal terms are given by

$$\langle T_{xy}\rangle = \frac{\partial}{\partial\rho_x}\frac{\partial}{\partial\rho_y} I[g(z)], \qquad \langle T_{0x}\rangle = i\frac{\partial}{\partial\tau}\frac{\partial}{\partial\rho_x} I[g(z)],$$
$$\langle T_{0y}\rangle = i\frac{\partial}{\partial\tau}\frac{\partial}{\partial\rho_y} I[g(z)], \tag{2.13e}$$

while

$$\langle T_{0z}\rangle = \langle T_{xz}\rangle = \langle T_{yz}\rangle = 0. \tag{2.13f}$$

III. ASYMPTOTIC BEHAVIOR

Now we wish to obtain a generalization of Eq. (1.6), which mirrors divergences much earlier obtained in curved space [16–18]. The large κ behavior to the integrand in (2.9) is dominated by that of the first term in Eq. (2.10). At coincident points, that term is approximated by the second WKB approximation [19]:

$$\frac{F(z)G(z)}{w} \sim \tilde{g}(z,z) \equiv \frac{1}{2\sqrt{\kappa^2+v(z)}} - \frac{v''(z)}{16(\kappa^2+v(z))^{5/2}} + \frac{5v'^2(z)}{64(\kappa^2+v(z))^{7/2}}. \tag{3.1}$$

In Eqs. (A8a) and (A8b), we have expanded $I[\tilde{g}]$ through order δ^2, thereby obtaining an approximation to $I[g]$ that is second order in both WKB and point-splitting senses. Inserting it into Eqs. (2.13), we obtain the stress tensor to second WKB order and to $O(\delta^0)$:

$$\begin{aligned}\langle\tilde{T}_{\mu\nu}\rangle = {}& \frac{1}{2\pi^2\delta^4}\begin{pmatrix} \frac{3\tau^2-\rho^2}{\delta^2} & \frac{4i\tau\rho_x}{\delta^2} & \frac{4i\tau\rho_y}{\delta^2} & 0 \\ \frac{4i\tau\rho_x}{\delta^2} & \frac{\tau^2+\rho_y^2-3\rho_x^2}{\delta^2} & \frac{4\rho_x\rho_y}{\delta^2} & 0 \\ \frac{4i\tau\rho_y}{\delta^2} & \frac{4\rho_x\rho_y}{\delta^2} & \frac{\tau^2+\rho_x^2-3\rho_y^2}{\delta^2} & 0 \\ 0 & 0 & 0 & 1 \end{pmatrix} + \frac{v(z)}{8\pi^2\delta^2}\begin{pmatrix} \frac{\rho^2-\tau^2}{\delta^2} & -\frac{2i\tau\rho_x}{\delta^2} & -\frac{2i\tau\rho_y}{\delta^2} & 0 \\ -\frac{2i\tau\rho_x}{\delta^2} & \frac{\rho_x^2-\tau^2-\rho_y^2}{\delta^2} & -\frac{2\rho_x\rho_y}{\delta^2} & 0 \\ -\frac{2i\tau\rho_y}{\delta^2} & -\frac{2\rho_x\rho_y}{\delta^2} & \frac{\rho_y^2-\rho_x^2-\tau^2}{\delta^2} & 0 \\ 0 & 0 & 0 & -1 \end{pmatrix} \\ & + \frac{v^2(z)}{32\pi^2}\left(\ln\frac{\sqrt{v}\delta}{2}+\gamma\right)\mathrm{diag}(1,-1,-1,-1) - \left(\xi-\frac{1}{6}\right)\frac{v''(z)}{8\pi^2}\left(\ln\frac{\sqrt{v}\delta}{2}+\gamma\right)\mathrm{diag}(1,-1,-1,0) \\ & + \frac{v^2(z)}{128\pi^2}\begin{pmatrix} \frac{\tau^2-3\rho^2}{\delta^2} & \frac{4i\tau\rho_x}{\delta^2} & \frac{4i\tau\rho_y}{\delta^2} & 0 \\ \frac{4i\tau\rho_x}{\delta^2} & \frac{3\tau^2+3\rho_y^2-\rho_x^2}{\delta^2} & \frac{4\rho_x\rho_y}{\delta^2} & 0 \\ \frac{4i\tau\rho_y}{\delta^2} & \frac{4\rho_x\rho_y}{\delta^2} & \frac{3\tau^2+3\rho_x^2-\rho_y^2}{\delta^2} & 0 \\ 0 & 0 & 0 & 3 \end{pmatrix} - \frac{v''(z)}{96\pi^2}\begin{pmatrix} \frac{\tau^2}{\delta^2} & \frac{i\tau\rho_x}{\delta^2} & \frac{i\tau\rho_y}{\delta^2} & 0 \\ \frac{i\tau\rho_x}{\delta^2} & -\frac{\rho_x^2}{\delta^2} & \frac{\rho_x\rho_y}{\delta^2} & 0 \\ \frac{i\tau\rho_y}{\delta^2} & \frac{\rho_x\rho_y}{\delta^2} & -\frac{\rho_y^2}{\delta^2} & 0 \\ 0 & 0 & 0 & 0 \end{pmatrix} \\ & + \frac{1}{96\pi^2}\left[6\frac{v'^2(z)}{v(z)} - \frac{\partial^2}{\partial z^2}\left(\frac{v''(z)}{v(z)}\right)\right]\mathrm{diag}(-\beta,\beta,\beta,1/4) \\ & + \frac{1}{384\pi^2}\left[\frac{v'^2(z)}{v(z)}\mathrm{diag}(-1,1,1,-5) + 2\frac{\partial^2}{\partial z^2}\left(\frac{v'^2(z)}{v^2(z)}\right)\mathrm{diag}(-\beta,\beta,\beta,1/4)\right]. \end{aligned} \tag{3.2}$$

(Here, the tilde notation means that the second WKB approximation is being employed.) Of the ten terms displayed above, the last two give the finite contribution from the final term in Eq. (3.1). The middle term in Eq. (3.1), which also arises from the second-order WKB approximation as discussed in Appendix A, contributes both to the eighth term in Eq. (3.2) and to the divergent and ambiguous terms proportional to v'', the sixth and fourth terms, and results in the conversion of β to the expected $\xi - 1/6$ in the fourth term above. The remaining terms arise from the zeroth-order WKB approximation, the first term in Eq. (3.1).

It is obvious that (at least) the most singular terms in Eq. (3.2) can be written in a covariant tensorial form in analogy to the formulas of Christensen [16] for the case of an external gravitational field. We find it convenient, however, to delay displaying the result of that step until after renormalization [see Eq. (5.11)].

IV. TRACE AND DIVERGENCE THEOREMS

From Eq. (1.3) we can immediately show, classically, that the trace of the stress tensor is

$$T^{\mu}{}_{\mu} = -v\phi^2 + \frac{1}{2}(6\xi-1)\partial^2\phi^2, \tag{4.1}$$

while the divergence is

$$\partial_\mu T^{\mu\nu} = -\frac{1}{2}\phi^2\partial^\nu v. \tag{4.2}$$

As expected, the stress tensor is conserved outside the potential region and is traceless there as well for conformal coupling, $\xi = 1/6$.

What happens quantum mechanically? Consider, first, the trace. According to Eqs. (2.13), the vacuum expectation value of the trace is

$$\begin{aligned}\langle T^\mu{}_\mu\rangle &= -\langle T^{00}\rangle + \langle T_{xx}\rangle + \langle T_{yy}\rangle + \langle T_{zz}\rangle \\ &= \left[-\left(\frac{\partial^2}{\partial\tau^2}+\frac{\partial^2}{\partial\rho_x^2}+\frac{\partial^2}{\partial\rho_y^2}\right)+\left(3\beta+\frac{1}{4}\right)\frac{\partial^2}{\partial z^2}\right]I[g] \\ &\quad - I[(\kappa^2+v)g].\end{aligned} \tag{4.3}$$

But $I[g]$ depends on the cutoff parameters only through the combination δ, so the above is simply

$$\begin{aligned}\langle T^\mu{}_\mu\rangle = -\left[\frac{\partial^2}{\partial\delta^2}+\frac{2}{\delta}\frac{\partial}{\partial\delta}-3\left(\xi-\frac{1}{6}\right)\frac{\partial^2}{\partial z^2}\right]I[g] \\ - I[(\kappa^2+v)g].\end{aligned} \tag{4.4}$$

Using

$$\left(-\frac{d^2}{d\delta^2}-\frac{2}{\delta}\frac{d}{d\delta}\right)\frac{\sin\kappa\delta}{\kappa\delta} = \kappa^2\frac{\sin\kappa\delta}{\kappa\delta}, \tag{4.5}$$

we simplify Eq. (4.4) to

$$\langle T^\mu{}_\mu\rangle = -vI[g] + 3\left(\xi-\frac{1}{6}\right)\partial_z^2 I[g], \tag{4.6}$$

which is the vacuum expectation value of the classical trace identity (4.1). This is true identically as a functional relationship for any g, so it is satisfied exactly by the WKB approximation, to any order.

What about the divergence equation (conservation law)? The nonzero component of the divergence of the stress tensor is

$$\partial_\mu\langle T^{\mu z}\rangle = \partial_z\langle T^{zz}\rangle = \frac{1}{4}\partial_z^3 I[g] - \partial_z I[(\kappa^2+v)g], \tag{4.7}$$

and the question is whether this is equal to $-\frac{v'}{2}I[g]$. This will be an identity if I is a functional of the exact Green's function which satisfies

$$(-\partial_z^2+\kappa^2+v)g(z,z') = 0, \qquad z\neq z'. \tag{4.8}$$

But the WKB approximants do not satisfy the equation of motion. In fact, if we use the zeroth-order approximation given in Eq. (3.2) (essentially the first seven terms there), we find that (terms that vanish with δ are omitted here and in the following),

$$\begin{aligned}\partial_z\langle\tilde{T}^{(0)}_{zz}\rangle + \frac{v'}{2}I[g^{(0)}] &= \frac{1}{4}\partial_z^3 I[g^{(0)}] - \partial_z I[(\kappa^2+v)g^{(0)}] \\ &\quad + \frac{v'}{2}I[g^{(0)}] = \partial_z\frac{1}{64\pi^2}\left(\frac{v'^2}{v}\right),\end{aligned} \tag{4.9}$$

where the right side is simply the z derivative of the unambiguous finite part of the stress tensor originating in this order, the first term in the penultimate line of Eq. (3.2), the seventh term. Note that this zeroth-order discrepancy is third order in derivatives. If we include both the zeroth- and second-order terms [all the terms displayed in Eq. (3.2)], the discrepancy is fifth order in derivatives,

$$\begin{aligned}&\frac{1}{4}\partial_z^3 I[g^{(0)+(2)}] - \partial_z I[(\kappa^2+v)g^{(0)+(2)}] + \frac{v'}{2}I[g^{(0)+(2)}] \\ &\quad = -\partial_z^3\frac{1}{384\pi^2}\left(\frac{v''}{v}-\frac{v'^2}{2v^2}\right) = \frac{1}{4}\partial_z^3 I[g^{(2)}],\end{aligned} \tag{4.10}$$

where $I[g^{(2)}]$ is given in Eq. (A8b). [Alternatively, it is the z derivative of the eight and tenth terms in Eq. (3.2).] If we go through the fourth order, we get

$$\begin{aligned}&\frac{1}{4}\partial_z^3 I[g^{(0)+(2)+(4)}] - \partial_z I[(\kappa^2+v)g^{(0)+(2)+(4)}] \\ &\quad + \frac{v'}{2}I[g^{(0)+(2)+(4)}] = \frac{1}{4}\partial_z^3 I[g^{(4)}],\end{aligned} \tag{4.11}$$

where $I[g^{(4)}]$ is given in Eq. (A8c). The discrepancy is now seventh order in derivatives. In each case, the lower-order discrepancy is canceled, and the remaining discrepancy is pushed to the next-higher order.

V. RENORMALIZATION

We now wish to obtain finite, "renormalized" values for $\langle\phi^2\rangle$ and $\langle T_{\mu\nu}\rangle$. The former is needed both to investigate the fate of the trace and divergence identities of Sec. IV and to provide a simple way of getting the renormalized stress tensor itself in parallel to the derivation of the regularized version (3.2); for the latter purpose, we need to keep the $O(\delta^2)$ terms in $I[g]$.

Naively, one would like simply to discard from (3.2) all terms that, as $\delta\to 0$, either diverge or depend on the direction of the point-splitting vector $(\tau,\boldsymbol{\rho})$. The problem of justifying that step physically by a genuine renormalization of coupling constants in a full theory including the gravitational field and the scalar field v as dynamical objects will not be discussed here (but see Refs. [9,12,13]); hence, our use of quotation marks around "renormalized." Another problem, however, cannot be postponed: It is impossible to separate logarithmically divergent terms from finite terms in a scale-invariant manner, and likewise it is impossible to separate direction-dependent terms from direction-independent finite terms unambiguously. Both

of these ambiguities afflict only the terms proportional to v^2 and v''; we shall refer to all such terms as being of "critical order." What is being confronted here is a close analogue of the situation in quantum field theory in curved spacetime that was resolved by intensive work in the late 1970s [15,20–22] (see also Ref. [23] and related papers), and we follow those references rather closely. The basic doctrine is that terms of critical order in the renormalized stress tensor are inherently ambiguous but can be constrained by certain physical requirements of conservation and covariance (tensoriality).

We start with the expression for $I[\tilde{g}] \equiv I[g^{(0)}] + I[g^{(2)}]$. Starting from Eqs. (A8a) and (A8b), we omit the $O(\delta^{-2})$ term and make the replacement

$$\ln\frac{\sqrt{v}\delta}{2} + \gamma - \frac{1}{2} \to \ln\frac{\sqrt{v}}{\mu}, \tag{5.1}$$

where μ is some arbitrary mass scale, in every logarithmic term. Note that the constant term on the left-hand side of rule (5.1) is an arbitrary convention, since a change in it can be regarded as a redefinition of μ, but it is important to adopt the same convention in every instance. The result is a tentatively renormalized expression:

$$4\pi^2\bar{I}_R[g^{(0)+(2)}] = \left[\frac{v}{2} + \frac{\delta^2}{16}\left(v^2 - \frac{1}{3}v''\right)\right]\ln\frac{\sqrt{v}}{\mu} - \frac{1}{24}\left(\frac{v''}{v} - \frac{1}{2}\frac{v'^2}{v^2}\right) - \frac{\delta^2}{64}\left(3v^2 + \frac{1}{3}\frac{v'^2}{v}\right), \tag{5.2}$$

in which the term $-\frac{3}{64}\delta^2 v^2$ arises because one logarithm in Eq. (A8a) has $-\frac{5}{4}$ instead of $-\frac{1}{2}$.

If Eq. (5.2) is inserted into Eqs. (2.13) in place of the unrenormalized $4\pi^2 I[g]$, one obtains a tentatively renormalized version of Eq. (3.2) from which all divergent or direction-dependent terms have disappeared. This calculation is facilitated by recognizing from Eq. (4.5) that Eq. (2.13d) may be replaced by

$$\langle T_{zz}\rangle = \left[\frac{1}{4}\partial_z^2 + \nabla_\delta^2 - v\right]I[g], \tag{5.3}$$

where we see the appearance of the Laplacian in the $\boldsymbol{\delta}$ coordinates, which on a spherically symmetric function becomes

$$\nabla_\delta^2 = \frac{\partial^2}{\partial\delta^2} + \frac{2}{\delta}\frac{\partial}{\partial\delta}. \tag{5.4}$$

In particular, $\nabla_\delta^2\delta^2 = 6$. However, it remains to grapple with the arbitrariness in the terms of critical order produced by this tentative procedure.

Adler *et al.* [18] and Wald [15,21] demanded that (in our terminology) the terms subtracted from $I[\tilde{g}]$ to yield $I_R[\tilde{g}]$ must themselves be the leading asymptotic terms of a certain minimal solution of the Green's function's differential equation. For technical reasons, we find it hard to follow Wald's procedure in our setting, but we offer a different physical argument that leads in the end to the same result, in the sense that our trace anomaly (5.10) agrees with Wald's general formula. We observe that all terms of critical order in the tentatively renormalized $\langle T_{\mu\nu}\rangle$ can be written tensorially in terms of the metric tensor and v and its covariant derivatives, with one exception, traceable to the term $-\frac{3}{64}\delta^2 v^2$ in $\bar{I}_R$ previously noted. The bad term in the stress tensor can be removed by modifying the critical-order terms in Eq. (5.2): $I_R \equiv \bar{I}_R + \Delta I_R$ with

$$4\pi^2\Delta I_R \equiv \frac{3}{64}\delta^2\left(v^2 - \frac{1}{3}v''\right). \tag{5.5}$$

Here we see the appearance of

$$a_2 = \frac{1}{2}\left(v^2 - \frac{1}{3}v''\right), \tag{5.6}$$

the second heat-kernel coefficient for the system under study ([24], Sec. 4.8; [25], chap. 9), which also occurs in the logarithmic term in Eq. (5.2). This gives a modification, for example, to the zz component of the stress tensor,

$$4\pi^2\Delta\langle T_{zz}\rangle = \frac{9}{16}a_2. \tag{5.7}$$

We now follow Wald [15] precisely, observing that the critical-order terms in the new renormalized stress tensor do not obey the conservation law (4.2):

$$4\pi^2\left[\partial_z\langle T_{zz}\rangle[I_R] + \frac{1}{2}v'I_R\right] = -\partial_z\frac{1}{16}a_2. \tag{5.8}$$

(This phenomenon is entirely separate from the WKB residual indicated in Eq. (4.10), which involves terms of higher order in derivatives and does not represent any anomaly in the exact stress tensor.) This "conservation anomaly" is cured by adding to the stress tensor another critical-order term:

$$\langle T^{\mu\nu}\rangle_R = \langle T^{\mu\nu}\rangle[I_R] + \frac{a_2}{64\pi^2}g^{\mu\nu}. \tag{5.9}$$

This step introduces a trace anomaly,

$$\langle T^\mu{}_\mu\rangle_R + vI_R - 3\left(\xi - \frac{1}{6}\right)\partial_z^2 I_R = \frac{1}{16\pi^2}a_2. \tag{5.10}$$

So with this set of redefinitions, we are finally led to the following form of the renormalized energy-momentum tensor,

$$4\pi^2\langle T^{\mu\nu}\rangle_R(z) = -g^{\mu\nu}\frac{v^2}{8}\ln\frac{\sqrt{v}}{\mu} - \frac{1}{2}\left(\beta+\frac{1}{12}\right)(\partial^\mu\partial^\nu - g^{\mu\nu}\partial^2)\left(v\ln\frac{\sqrt{v}}{\mu}\right) + g^{\mu\nu}\frac{v^2}{32} + \frac{1}{96}\frac{v'^2}{v}\,\mathrm{diag}(1,-1,-1,1) - \frac{1}{24}\partial_z^2\left(\frac{v''}{v} - \frac{1}{2}\frac{v'^2}{v^2}\right)\mathrm{diag}\left(-\beta,\beta,\beta,\frac{1}{4}\right) + 4\pi^2 t^{\mu\nu}, \tag{5.11}$$

where $t^{\mu\nu}$ is the remainder of the stress tensor, obtained by the construction in Eqs. (2.13) when the zeroth and second WKB approximations are subtracted from the Green's function,

$$t^{\mu\nu} = \langle T^{\mu\nu}\rangle - \langle\tilde{T}^{\mu\nu}\rangle = \langle T^{\mu\nu}\rangle[I[g-\tilde{g}]]. \tag{5.12}$$

The form of the renormalized stress tensor (5.11) is a central result of this paper.

Note that the terms of critical order [in the top line of Eq. (5.11)] are now completely tensorial. The terms in the second line are, strictly speaking, part of the finite remainder, which need not be covariant in that sense. Note also that the off-diagonal tensor components, which in Eq. (3.2) were entirely direction-dependent, have now completely disappeared. The direction-independent off-diagonal finite terms must vanish by reflection symmetry in each of the coordinates t, x, and y. The renormalized $\langle T_{xx}\rangle_R$ and $\langle T_{yy}\rangle_R$ are the same as $u_R = \langle T^{00}\rangle_R$, except for a reversal of sign; see Eqs. (2.13b) and (2.13c). This proves the nonexistence of a transverse pressure anomaly [13], completing the argument in Ref. [11].

We will compute $t^{\mu\nu}$ numerically in the following two sections, for a linear and a quadratic potential, respectively, where explicit formulas for the exact Green's functions can be given.

VI. ENERGY DENSITY FOR THE LINEAR WALL

Let us consider the energy density for the linear wall, within the region of the potential,

$$z>0:\ v(z)=z. \tag{6.1}$$

In this case, the renormalized WKB stess tensor (5.11) gives the leading contribution:

$$\tilde{u}_R = \langle\tilde{T}^{00}\rangle_R = \frac{1}{32\pi^2}z^2\left(\ln\frac{\sqrt{z}}{\mu}-\frac{1}{4}\right) - \frac{\beta}{16\pi^2 z} - \frac{1}{384\pi^2}\left[\frac{1}{z}+\frac{12\beta}{z^4}\right]. \tag{6.2}$$

The remainder of the energy density comes from substituting $g-\tilde{g}$ into Eq. (2.9) and using the construction for the energy density in terms of this vacuum-expectation value, Eq. (2.13a). Since the integral defining the remainder is convergent without the cutoff, we expand the cutoff factor, $\sin\kappa\delta/(\kappa\delta) = 1-(\kappa\delta)^2/6+\cdots$, and obtain the remainder:

$$(u-\tilde{u})(z) = -\frac{1}{2\pi^2}\int_0^\infty d\kappa\kappa^2\left(\frac{1}{3}\kappa^2+\beta\frac{\partial^2}{\partial z^2}\right)\times[g(z,z)-\tilde{g}(z,z)]. \tag{6.3}$$

Here, the explicit Green's function for the linear potential is

$$g(z,z) = \pi\mathrm{Ai}(\kappa^2+z)\mathrm{Bi}(\kappa^2+z) - \frac{(\kappa\mathrm{Bi}-\mathrm{Bi}')(\kappa^2)}{(\kappa\mathrm{Ai}-\mathrm{Ai}')(\kappa^2)}\pi\mathrm{Ai}^2(\kappa^2+z). \tag{6.4}$$

We know from Ref. [11] that the WKB approximation is quite good for large κ, so the integral (6.3) should converge quite rapidly. The integrand is plotted in Fig. 1. To the numerical integration of the remainder (6.3), we add the portion of the renormalized WKB energy from Eq. (6.2) that dominates for small values of z,

$$u_{\mathrm{wkb}} = -\frac{1}{384\pi^2}\left(\frac{1+24\beta}{z}+\frac{12\beta}{z^4}\right). \tag{6.5}$$

(The dominant terms in the renormalized energy density for large distances,

$$u_{\mathrm{leading}} = \frac{1}{32\pi^2}z^2\left(\ln\frac{\sqrt{z}}{\mu}-\frac{1}{4}\right), \tag{6.6}$$

are ambiguous because they depend on the arbitrary scale μ, and require further discussion.) In Fig. 2, we plot the sum $u-\tilde{u}+u_{\mathrm{wkb}}$, which we call the "residual energy density." It is seen that in each case the residual energy density

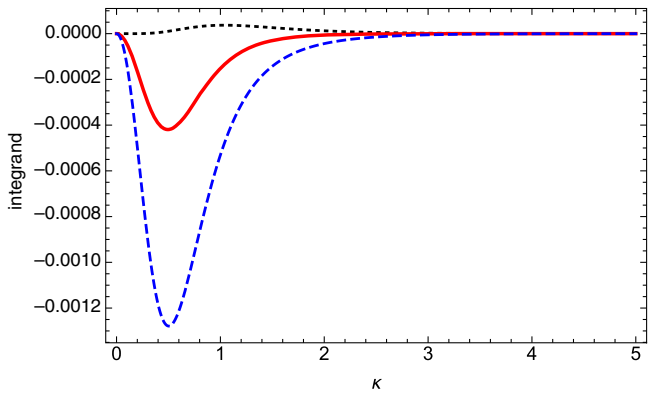

FIG. 1. Integrand in Eq. (6.3) for $z=1$ for $\beta=0$ (dotted), $\beta=-1/12$, the conformal value (thick), and $\beta=-1/4$ (dashed). (All figures were prepared with *Mathematica*.)

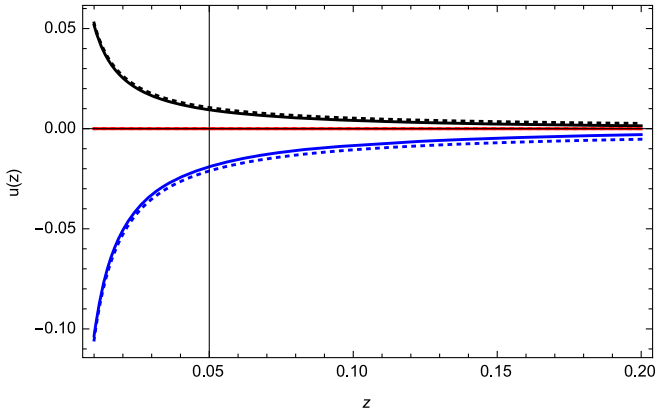

FIG. 2. Residual energy density within the wall for a linear potential. The solid curves show, from top to bottom, the energy density for $\beta = 0, -1/12, -1/4$, compared with the dotted curves which show the surface energy estimates from Eq. (6.7).

rapidly goes to zero as $z \to \infty$. (Of course, the terms in u_{leading}, Eq. (6.6), grow for large z.) For the conformal case, $\beta = -1/12$, the energy density is nearly zero. Otherwise, the energy diverges as the boundary $z = 0$ is approached. For $\beta < -1/12$ the residual energy is everywhere negative, while for $\beta > -1/12$ the energy density is positive. The leading WKB divergence seen in Eq. (6.5), going like z^{-4}, is clearly spurious, being canceled by the remainder energy density (6.3). Thus, the dominant structure in the integrand seen in Fig. 1 reflects this ultimately spurious behavior, and the integrations have to be carried out to much higher values of κ than Fig. 1 suggests. The remaining divergence near the boundary is precisely the same (in terms of $|z|$) as found in Ref. [10] for the exterior region [see our Eq. (1.4)]

$$u_{\text{surf}} = \frac{1 + 12\beta}{192\pi^2 z}. \tag{6.7}$$

This is shown as the dotted curves in Fig. 2. In Appendix B, we give a plausibility argument for why this result might have been expected.

VII. ENERGY DENSITY FOR THE QUADRATIC WALL

Now we are looking at

$$v(z) = z^2, \qquad \alpha = 2, \tag{7.1}$$

for which the renormalized second-order WKB energy density is

$$\tilde{u}_R = \langle \tilde{T}^{00} \rangle_R = \frac{z^4}{32\pi^2}\left(\ln\frac{z}{\mu} - \frac{1}{4}\right) - \frac{\xi - 1/6}{4\pi^2}\ln\frac{z}{\mu} - \frac{1}{48\pi^2}(1 + 18\beta). \tag{7.2}$$

The remainder of the energy density is given by

$$(u - \tilde{u})(z) = -\frac{1}{2\pi^2}\int_0^\infty d\kappa\kappa^2\left(\frac{\kappa^2}{3} + \beta\frac{\partial^2}{\partial z^2}\right) \times \left[g(z,z) - \frac{1}{2\sqrt{\kappa^2 + z^2}} + \frac{1}{8(\kappa^2 + z^2)^{5/2}} - \frac{5}{16}\frac{z^2}{(\kappa^2 + z^2)^{7/2}}\right]. \tag{7.3}$$

The diagonal Green's function for the quadratic wall is

$$g(z,z) = \frac{\Gamma(\frac{\kappa^2+1}{4})\Gamma(\frac{\kappa^2+3}{4})}{\pi 2^{(3-\kappa^2)/2}}\left[D_{-\frac{\kappa^2+1}{2}}(\sqrt{2}z)D_{-\frac{\kappa^2+1}{2}}(-\sqrt{2}z) - \frac{\Gamma(\frac{\kappa^2+1}{4}) - \frac{2}{\kappa}\Gamma(\frac{\kappa^2+3}{4})}{\Gamma(\frac{\kappa^2+1}{4}) + \frac{2}{\kappa}\Gamma(\frac{\kappa^2+3}{4})}D^2_{-\frac{\kappa^2+1}{2}}(\sqrt{2}z)\right], \tag{7.4}$$

in terms of parabolic cylinder functions. The WKB approximation is very accurate, as shown in Fig. 3.

This time we add to the remainder energy, computed numerically, the parts of the renormalized WKB energy (7.2) important for small z,

$$u_{\text{wkb}} = -\frac{1 + 12\beta}{48\pi^2}\ln\frac{z}{\mu} - \frac{1}{48\pi^2}(1 + 18\beta). \tag{7.5}$$

(Again, we omit the leading term in the renormalized WKB energy

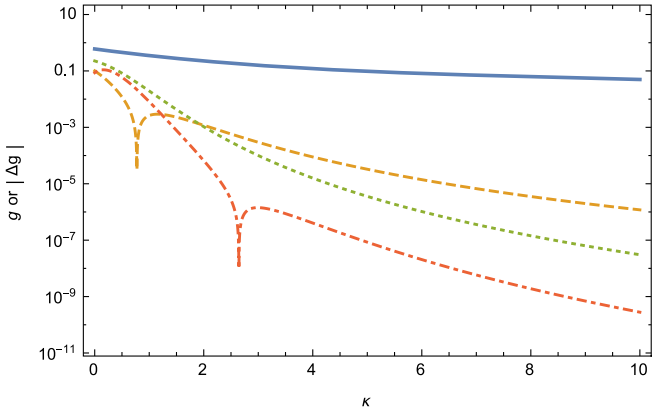

FIG. 3. The reduced diagonal Green's function for the quadratic wall, for $z = 1$, shown by the solid curve. The dashed curve shows the absolute value of the residual Green's function after the leading WKB approximation is removed, the dotted curve shows the residual after the two leading WKB approximations are subtracted, and the dot-dashed curve shows the absolute value of the residual after the first three WKB approximations shown in Eq. (7.3) are subtracted (top to bottom on the right). Thus the bottom curve shows the effect of subtracting the WKB approximations through second order. (Because what is plotted is the logarithm of the absolute value of the residual of $g(z,z)$, the spikes occur at the points where the differences change sign.)

$$u_{\text{leading}} = \frac{z^4}{32\pi^2}\left(\ln\frac{z}{\mu} - \frac{1}{4}\right) \tag{7.6}$$

which is dominant for large distances.) Convergence of the integral for the remainder energy is quite slow in this case, complicated by the fact that *Mathematica* fails to compute the parabolic cylinder function accurately for large κ. Therefore, it is necessary to break up the integration into two parts,

$$u(z) = \int_0^K d\kappa \mathcal{I}(\kappa, z) + \int_K^\infty d\kappa \mathcal{I}(\kappa, z), \tag{7.7}$$

where $\mathcal{I}$ is the integrand shown in Eq. (7.3), and then compute the second integral, for large K, from the dominant WKB approximation coming from the second term in Eq. (2.10) [see Appendix B, Eq. (B11)],

$$g_{F^2} \sim \frac{1}{16\kappa^5} e^{-2\kappa z}, \qquad \kappa \to \infty, \tag{7.8}$$

which leads to the approximate evaluation,

$$\mathcal{I}(\kappa, z) \sim -\frac{1+12\beta}{96\pi^2}\frac{1}{\kappa} e^{-2\kappa z}, \qquad \kappa \to \infty, \tag{7.9}$$

and then to a form for the energy density suitable for numerical calculation,

$$(u - \tilde{u})(z) \approx \int_0^K d\kappa \mathcal{I}(\kappa, z) - \frac{1+12\beta}{96\pi^2}\Gamma(0, 2Kz), \tag{7.10}$$

in terms of the incomplete gamma function. Figure 4 shows the residual energy density composed of the remainder energy (7.3) [computed using Eq. (7.10)] plus u_{wkb} [from Eq. (7.5)] for $\beta = 0, -1/12$ (the conformal value), $-1/4$, and $1/20$. The method of Appendix B yields a surface term,

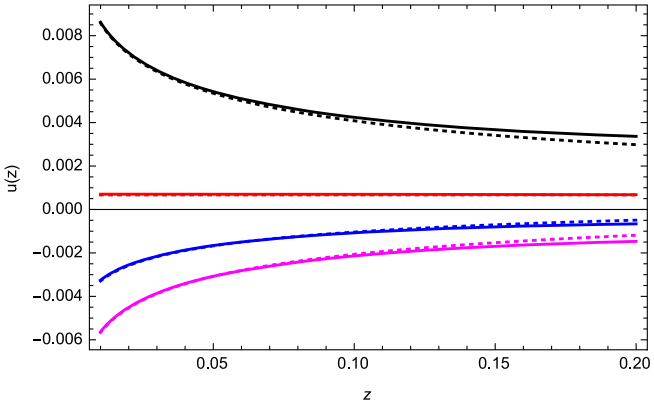

FIG. 4. Numerical integration of the residual energy [the sum of Eqs. (7.3) plus (7.5)] for the quadratic wall for $\beta = 1/20$, $\beta = 0$, $\beta = -1/12$, the conformal value, and $\beta = -1/4$, from bottom to top. The results are insensitive to the value of K, as long as it is sufficiently large, but not so large that the errors in computing parabolic cylinder functions are significant. Here we used $K = 10$. Here μ is arbitrarily taken to be 1. The dotted curves are the surface energies (7.11) with the offset (7.12).

$$u_{\text{surf}} = -\frac{1+12\beta}{96\pi^2}\Gamma(0, 2z), \tag{7.11}$$

which is, in fact, the same as the exterior result, Eq. (1.5), except, this time, for sign. However, a constant term is undetermined by our asymptotic analyses. To match the data, the surface energy is shifted by a constant amount, which is empirically fitted by the simple formula:

$$u_{\text{offset}} = 0.00025(1 - 20\beta). \tag{7.12}$$

(The value for $\beta = 1/20$ is shown in the graph to demonstrate that no offset is required in that case.) The fit is quite remarkably good. The numerical fit, for large κ and small z, is the statement

$$\int_0^K d\kappa \mathcal{I}(\kappa, z) - \frac{1+12\beta}{48\pi^2}\ln z - \frac{1+18\beta}{48\pi^2} + \frac{1+12\beta}{96\pi^2}[\Gamma(0, 2z) - \Gamma(0, 2Kz)] \approx 0.00025(1 - 20\beta). \tag{7.13}$$

VIII. OTHER STRESS TENSOR COMPONENTS

As noted above, $\langle T^{\mu\nu}\rangle_R$ is diagonal, and

$$\langle T_{xx}\rangle_R = \langle T_{yy}\rangle_R = -u_R. \tag{8.1}$$

So we only have to examine $\langle T_{zz}\rangle_R$.

For the linear wall, the second-order renormalized WKB stress tensor (5.11) gives for the linear potential (omitting the ambiguous leading term

$$T_{zz}^{\text{leading}} = -\frac{z^2}{32\pi^2}\left(\ln\frac{\sqrt{z}}{\mu} - \frac{1}{4}\right), \tag{8.2}$$

which is irrelevant for small z)

$$\langle T_{zz}\rangle_{\text{wkb}} = \frac{1}{384\pi^2}\left(\frac{1}{z} + \frac{3}{z^4}\right). \tag{8.3}$$

This is added to the numerical evaluation of the remainder,

$$t_{zz} = \langle T_{zz}\rangle - \langle \tilde{T}_{zz}\rangle = \frac{1}{2\pi^2}\int_0^\infty d\kappa\kappa^2\left(\frac{1}{4}\frac{\partial^2}{\partial z^2} - (\kappa^2 + z)\right) \times \left[g(z, z) - \frac{1}{2\sqrt{\kappa^2 + z}} - \frac{5}{64(\kappa^2 + z)^{7/2}}\right], \tag{8.4}$$

and $t_{zz} + \langle T_{zz}\rangle_{\text{wkb}}$ is shown in Fig. 5. Now there is no surface divergence, and the residual stress tensor within the wall [leaving aside the contribution of Eq. (8.2)] is very small. (The corresponding stress tensor outside the wall is exactly zero [10,11].)

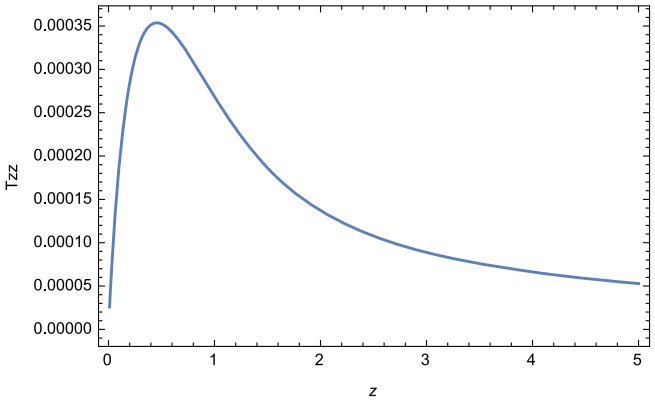

FIG. 5. This shows the numerical values of the remainder (8.4) added to the WKB approximation (8.3) for the zz component of the stress tensor within the wall, for a linear potential. The surface divergences apparent in the WKB approximation are completely canceled out by the numerical remainder, leaving only a small residual.

As for the trace and divergence identities, Eqs. (5.10) and (5.8), these are not modified by the residual finite contributions. The former is structurally true as noted in Eq. (4.6). The latter should be respected because the modification of the stress tensor (5.9) involved only the critical terms. We have checked numerically that our approximations are consistent,

$$4\pi^2\left[\partial_z t_{zz}+\frac{v'}{2}(I-\tilde{I})\right]-\frac{1}{96}\partial_z^3\left(\frac{v''}{v}-\frac{v'^2}{2v^2}\right)$$
$$\to 2\int_0^\infty d\kappa\kappa^2\left[\frac{1}{4}\partial_z^3-(\kappa^2+z)\partial_z-\frac{1}{2}\right](g-\tilde{g})-\frac{1}{8z^5}\approx 0, \tag{8.5}$$

consistent with zero within machine precision, where the substitution is for the linear wall. Numerical consistency of the remainder stress tensor with the divergence identity has been verified also for the quadratic wall.

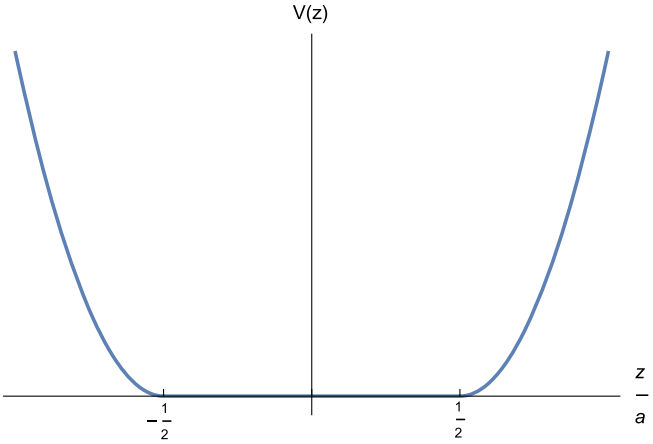

FIG. 6. Two facing soft walls, each modeled by a potential $v(z)$, separated by a distance a. The origin is chosen at the midpoint between the two facing potentials.

IX. INTERACTION BETWEEN TWO MIRRORED SOFT WALLS

Now imagine we have two such soft walls separated by a distance a, as shown in Fig. 6. That is, let the potential be

$$V(z)=\begin{cases} v(-z-a/2), & z<-a/2,\\ 0, & -a/2<z<a/2,\\ v(z-a/2), & a/2<z.\end{cases} \tag{9.1}$$

There is a Casimir force between the walls, and because each wall can move without changing its shape, it should be possible to calculate this force without depending upon the renormalization theory developed in the previous sections for the region inside the potential. This indeed turns out to be the case.

The reduced Green's function satisfies

$$\left(-\frac{\partial^2}{\partial z^2}+\kappa^2+V(z)\right)g(z,z')=\delta(z-z'), \tag{9.2}$$

which has the following solution in the three regions:

$$z<-a/2:\ g(z,z')=\frac{1}{w}F(-z_<-a/2)G(-z_>-a/2)+R\frac{1}{w}F(-z-a/2)F(-z'-a/2), \tag{9.3a}$$

$$-a/2<z<a/2:\ g(z,z')=\frac{1}{2\kappa}e^{-\kappa|z-z'|}+\frac{1}{2\kappa}\frac{2r}{e^{2\kappa a}-r^2}[r\cosh\kappa(z-z')+e^{\kappa a}\cosh\kappa(z+z')], \tag{9.3b}$$

$$z>a/2:\ g(z,z')=\frac{1}{w}F(z_>-a/2)G(z_<-a/2)+R\frac{1}{w}F(z-a/2)F(z'-a/2). \tag{9.3c}$$

Here F and G are independent solutions of the single potential problem (2.11), with, again, F being the solution that vanishes at $z=+\infty$. Because the potential defines a cavity, in this section, we will refer to the solutions F, G as the "exterior" solutions, while the exponential solutions within the cavity are referred to as "interior." The Wronskian of the two exterior solutions is w, Eq. (2.12), is independent of z, and subsumes any normalization

condition. The reflection coefficients here are generically computed by multiple scattering. In terms of the abbreviations,

$$F_\pm = \kappa F(0) \pm F'(0), \qquad G_\pm = \kappa G(0) \pm G'(0), \tag{9.4}$$

the interior (within the cavity) reflection coefficient is

$$r = \frac{F_+}{F_-} < 1, \tag{9.5}$$

as already seen in Ref. [10].

The exterior (outside the cavity) reflection coefficient R is composed of the single-wall exterior reflection coefficient $\bar{r}$,

$$\bar{r} = -\frac{G_-}{F_-}, \tag{9.6}$$

also as given in Ref. [10], followed by multiple reflections between the interior walls,

$$R = \bar{r} + \frac{rt^2}{e^{2\kappa a} - r^2}, \tag{9.7}$$

which involves the transmission coefficient across the wall (the same in either direction),

$$t = \frac{\sqrt{2\kappa w}}{F_-}, \tag{9.8}$$

where the numerator refers to the Wronskian w for the exterior solutions (F, G) and the Wronskian (2κ) for the interior solutions $(e^{\pm\kappa z})$. Under an arbitrary scaling of the solutions, $F \to mF$, $G \to nG$, where m and n are constants, the Wronskian changes by $w \to mnw$, the interior reflection coefficient does not change, $r \to r$, while the exterior reflection coefficient and transmission coefficient change,

$$\bar{r} \to \frac{n}{m}\bar{r}, \qquad t \to \sqrt{\frac{n}{m}}t, \tag{9.9}$$

and hence the total reflection coefficient R changes in the same way as $\bar{r}$: $R \to \frac{n}{m}R$, thus verifying the scaling consistency of Eq. (9.8).

Using only the interior reflection coefficient r, it is easy to calculate the zz component of the stress tensor in the vacuum region between the potentials, $-a/2 < z < a/2$, using the prescription (2.13d). The (divergent) contribution from the first term in Eq. (9.3b), $1/(2\kappa)e^{-\kappa|z-z'|}$, is recognized as the universal zero-point pressure and discarded. [This corresponds to the T_{zz} component of the first term in Eq. (3.2).] The remainder leads immediately to the Lifshitz formula [2],

$$t_{zz} = P = -\frac{1}{2\pi^2}\int_0^\infty d\kappa\kappa^3 \frac{1}{r^{-2}e^{2\kappa a} - 1}, \tag{9.10}$$

which is independent of where it is evaluated in the cavity.

If there is no additional pressure exerted on the system from infinity, P is pressure felt by each wall; it is attractive, as expected. In earlier sections, however, we have found terms in the renormalized stress tensor that grow as $|z| \to \infty$; the interpretation of these presumably unphysical terms is a topic for future work.

We now wish to verify the principle of virtual work in the longitudinal direction, that is, that this pressure is the negative derivative of the total energy of the system with respect to the distance between the walls,

$$P = -\frac{\partial U}{\partial a}, \tag{9.11}$$

where U is the integral of the energy density over the entire system, the energy per unit area,

$$U = \int_{-\infty}^\infty dz u(z), \tag{9.12}$$

where u is obtained by the operations given in Eq. (2.13a). The term proportional to β vanishes because it is a total derivative; there is no dependence on the conformal parameter in the total energy. Then, temporarily ignoring the first terms in each of Eqs. (9.3), we calculate

$$U - U_0 = -\frac{1}{6\pi^2}\int_0^\infty d\kappa\kappa^4 \left[\frac{2R}{w}\int_0^\infty dz F^2(z) + \frac{1}{2\kappa}\frac{r}{e^{2\kappa a} - r^2}\left(2ra + \frac{1}{\kappa}(e^{2\kappa a} - 1)\right)\right]. \tag{9.13}$$

The contribution U_0 of the ignored terms is divergent but can indeed be ignored, for the following reasons. The two integrals stemming from Eqs. (9.3a) and (9.3c) are formally independent of a, in accordance with our intuition that the self-energies of the walls are irrelevant to the force. The contribution from the first term in Eq. (9.3b) appears to be proportional to a, but again, we know from Refs. [10,11] that this term is precisely the bulk zero-point energy inside the gap.

Even though we do not have an explicit expression for the fundamental solution F, the first integral in Eq. (9.13) can be evaluated just from the differential equation satisfied by F, as shown in Ref. [26]:

$$\int_0^\infty dz F^2(z) = \frac{1}{2\kappa}F(0)F'(0)\frac{d}{d\kappa}\ln\frac{F(0)}{F'(0)}. \tag{9.14}$$

The latter may be readily expressed in terms of the reflection coefficient r:

$$\int_0^\infty dz F^2(z) = -\frac{F_-^2}{(2\kappa)^2}\left(\frac{r^2-1}{2\kappa}+\frac{dr}{d\kappa}\right). \tag{9.15}$$

When this is substituted into Eq. (9.13), and terms independent of a omitted, we obtain

$$\begin{aligned} U &\to -\frac{1}{12\pi^2}\int_0^\infty d\kappa\kappa^3 \frac{1}{e^{2\kappa a}-r^2}\left[-2r\frac{dr}{d\kappa}+2r^2 a\right] \\ &= \frac{1}{4\pi^2}\int_0^\infty d\kappa\kappa^2 \ln\left(1-r^2e^{-2\kappa a}\right), \end{aligned} \tag{9.16}$$

where the last step involves integration by parts. Evidently, differentiating this with respect to $-a$ yields the pressure (9.10); that is, Eq. (9.11) is satisfied.

As noted at the beginning, the Green's function is invariant under the substitution $G \to G + pF$, where p is independent of z. Here p is not allowed to depend on the separation between the walls. Such a substitution does not change the Wronskian or the transmission coefficient, but does change the reflection coefficient by a constant, $R \to R - p$. Therefore, the energy (9.13) changes only by a constant, and the Casimir pressure on one wall is unchanged.

X. CONCLUSION

We have, in this paper, significantly extended the analysis given in Ref. [10]. We now have extracted all the divergences corresponding to the soft-wall potential and have computed the energy density and stress tensor within as well as outside the region of the potential, for the case of linear and quadratic potentials. The renormalized energy density exhibits divergences as the boundary is approached, just as it does in the case of a Dirichlet wall, but much weaker; these divergences are the same (up to a sign) on both sides of the wall. The fact that the surface divergences are proportional to $\xi - \frac{1}{6}$ indicates the irrelevance of these terms, since the total energy must be independent of the conformal parameter. However, before we can ascribe a finite self-energy to this configuration, we must recognize that terms in the energy density that grow with the distance into the wall require physical interpretation. It may be that the only physically unambiguously observable consequence is the force between two soft walls, which we calculated in the last section of this paper.

In future work, we hope to further understand the meaning of the energy density, total energy, and stress in these configurations. We hope to make progress in solving the problem for general α: In particular, the limit of $\alpha \to \infty$ would be of great interest to study, because that limit would correspond to the appearance of a hard Dirichlet wall at $z = 1$. (The emergence of this preferred length scale in a seemingly scale-invariant problem is related to the coupling constant that we have suppressed, as explained in Ref. [9].) As α grows, the WKB approximation becomes increasingly unsuited to the region of small κ and z, and hence it will be necessary to bring in approximations at small κ, completing the program of Ref. [11]. Accurate treatment of the contributions to the energy density from small κ should clarify and remedy the deficiencies in the analysis offered in Appendix B.

ACKNOWLEDGMENTS

The work of K. A. M. was supported in part by a grant from the Julian Schwinger Foundation. We thank Li Yang, Alex Mau, and Jacob Tice for collaborative assistance, and Steve Christensen, Itay Griniasty, and Ulf Leonhardt for helpful conversations.

APPENDIX A: WKB APPROXIMATION

In the text, we are considering approximate solutions to the problem

$$y''(z) = Q(z)y(z), \qquad Q(z) = \kappa^2 + v(z), \tag{A1}$$

with Q positive and large. The effective expansion parameter, therefore, multiplies Q as a whole; one can write $\epsilon^2 y'' = Qy$, $\epsilon \to 0$. (In quantum mechanics, ϵ is identified with Planck's constant.) We suppress ϵ (take it equal to 1) in the detailed formulas.

The WKB approximation is constructed to high order in [19] in terms of local functionals of Q, which we denote q_n, for each non-negative integer n:

$$y(z) \sim \exp\left[\epsilon^{-1}\sum_{n=0}^{\infty}(\pm)\int^z \epsilon^n q_n(t)dt\right]. \tag{A2}$$

Fröman [27] noted that the odd-order terms can be resummed into the prefactor:

$$\begin{aligned} y(z) \sim{}& \frac{1}{\sqrt{q_0(z)+q_2(z)+q_4(z)+\cdots}} \\ &\times e^{\pm\int^z dt[q_0(t)+q_2(t)+q_4(t)+\cdots]}, \end{aligned} \tag{A3}$$

where q_n is accompanied by ϵ^{n-1} in the exponent and by ϵ^n in the prefactor. The first three even-order WKB integrands are (in the notation of Bender and Orszag [19])

$$q_0(t) = Q^{1/2}(t), \tag{A4a}$$

$$q_2(t) = \frac{Q''(t)}{8Q^{3/2}(t)} - \frac{5}{32}\frac{Q'^2}{Q^{5/2}(t)}, \tag{A4b}$$

$$\begin{aligned} q_4(t) = {}& \frac{Q^{(4)}(t)}{32Q^{5/2}(t)} - \frac{7}{32}\frac{Q'(t)Q'''(t)}{Q^{7/2}(t)} - \frac{19}{128}\frac{Q''^2(t)}{Q^{7/2}(t)} \\ &+ \frac{221}{256}\frac{Q''(t)Q'^2(t)}{Q^{9/2}(t)} - \frac{1105}{2048}\frac{Q'^4(t)}{Q^{11/2}(t)}. \end{aligned} \tag{A4c}$$

(In Ref. [27], Q is called Q^2.) In the Fröman approximation of order $2n$, the exponential sum terminates with q_{2n} and the prefactor sum terminates with q_{2n-2}. In the approximation of order $2n+1$, both series extend through q_{2n}.

When these successive WKB approximants are used in computing the first term in the diagonal Green's function (2.10), orders $2n$ and $2n+1$ give identical results for the particular combination that is relevant,

$$\frac{F(z)G(z)}{w} = \left(\frac{G'(z)}{G(z)} - \frac{F'(z)}{F(z)}\right)^{-1} \sim \frac{1}{2}\frac{1}{q_0+q_2+q_4+\cdots}. \tag{A5}$$

(Recall that F is the solution which vanishes exponentially at positive infinity, so G must be dominated by the exponentially growing solution.) Continuing to expand in powers of ϵ,

$$\frac{FG}{w}(z) \sim \frac{1}{2q_0(z)}\left(1 - \frac{q_2(z)}{q_0(z)} + \left[\left(\frac{q_2(z)}{q_0(z)}\right)^2 - \frac{q_4(z)}{q_0(z)}\right] + O(\epsilon^6)\right). \tag{A6}$$

The zeroth-order WKB term yields the first term displayed in Eq. (3.1), while the second and third terms there result from the second-order term in Eq. (A6). The two terms in the square brackets in Eq. (A6) give the fourth-order contribution to the coincident Green's function,

$$g^{(4)}(z,z) = \frac{1}{2\sqrt{Q}}\left(-\frac{1}{32}\frac{v^{(4)}}{Q^3} + \frac{7}{32}\frac{v'v'''}{Q^4} + \frac{21}{128}\frac{v''^2}{Q^4} - \frac{231}{256}\frac{v''v'^2}{Q^5} + \frac{1155}{2048}\frac{v'^4}{Q^6}\right). \tag{A7}$$

Note that an expansion in ϵ is not quite the same thing as one in $1/\kappa$. Including enough WKB terms is sufficient but not necessary to obtain a certain order in κ. Thus, in Eq. (3.1), the second term was necessary to capture all divergences [10], whereas the third term was not but is needed to capture the correct WKB behavior at large z.

To compute all the components of the stress tensor, we have to expand $I[g]$ out to order δ^2. The corresponding terms are

$$4\pi^2 I[g^{(0)}] = \frac{1}{\delta^2} + \frac{v}{2}\left(\ln\frac{\sqrt{v}\delta}{2} + \gamma - \frac{1}{2}\right) + \frac{v^2\delta^2}{16}\left(\ln\frac{\sqrt{v}\delta}{2} + \gamma - \frac{5}{4}\right), \tag{A8a}$$

$$4\pi^2 I[g^{(2)}] = \frac{1}{24}\left(-\frac{v''}{v} + \frac{1}{2}\frac{v'^2}{v^2}\right) - \frac{v''\delta^2}{48}\left(\ln\frac{\sqrt{v}\delta}{2} + \gamma - \frac{1}{2}\right) - \frac{\delta^2}{192}\frac{v'^2}{v}, \tag{A8b}$$

$$4\pi^2 I[g^{(4)}] = -\frac{1}{240}\frac{v^{(4)}}{v^2} + \frac{1}{60}\frac{v'v''}{v^3} + \frac{1}{80}\frac{v''^2}{v^3} - \frac{11}{240}\frac{v'^2v''}{v^4} + \frac{1}{48}\frac{v'^4}{v^5} + \delta^2\left[\frac{1}{960}\frac{v^{(4)}}{v} - \frac{1}{480}\frac{v'v'''}{v^2} - \frac{1}{640}\frac{v''^2}{v^2} + \frac{11}{2880}\frac{v''v'^2}{v^3} - \frac{1}{768}\frac{v'^4}{v^4}\right]. \tag{A8c}$$

APPENDIX B: "SURFACE" DIVERGENCE

Here we examine the behavior of the energy as the boundary at $z=0$ is approached from above. We confine attention to the cases of interest in this paper, $\alpha = 1$ and 2, and to the contribution from the WKB region of the Euclideanized spectrum, which appears to be the most important one.

Recall that the Green's function has the construction [see Eqs. (2.10)–(2.12) and (9.4)]

$$z, z' > 0\colon\ g(z,z') = \frac{1}{w}F(z_>)G(z_<) - \frac{G_-}{F_-}\frac{1}{w}F(z)F(z'), \tag{B1a}$$

$$z, z' < 0\colon\ g(z,z') = \frac{1}{2\kappa}e^{-\kappa(z_>-z_<)} + \frac{F_+}{F_-}\frac{1}{2\kappa}e^{\kappa(z+z')}. \tag{B1b}$$

When $z' = z > 0$, we introduce a short notation for the two terms in Eq. (B1a),

$$g_{FG} = \frac{1}{w}F(z)G(z), \qquad g_{FF} = -\frac{1}{w}\frac{G_-}{F_-}F(z)^2. \tag{B2}$$

In the case $\alpha = 1$ (the linear wall), the exponentially decreasing solution F can be chosen as $\mathrm{Ai}(\kappa^2+z)$, and the independent solution G can be chosen as $\mathrm{Bi}(\kappa^2+z)$.

In Secs. III and VI, we used the WKB approximation only on the first term in Eq. (B1a). As we have seen, although it captures the correct behavior for large κ, this procedure generates spurious singularities for z near the boundary, presumably stemming from the inadequacy of the WKB approximation at small κ and the neglect of the second term, g_{FF}. We argue that this first term is, in fact, not

relevant to the question of "surface divergences." The corresponding energy density is given by

$$u_{FG} = \left(\frac{\partial^2}{\partial\tau^2} - \beta\frac{\partial^2}{\partial z^2}\right) I[g_{FG}]. \tag{B3}$$

For $\alpha = 1$, the explicit form of g_{FG} appears as the first term in Eq. (6.4). Use of the asymptotic expansions of the Airy functions for large argument gives, of course, the WKB result (6.2). But suppose, on the contrary, that we simply subtract (even at positive z) the first term in Eq. (B1b), which would produce the free-field zero-point energy. That is, we replace g_{FG} by $g_{FG} - 1/(2\kappa)$. Then one can easily check numerically that $I[g_{FG} - 1/(2\kappa)]$ has a finite second derivative with respect to τ for $z \to 0$ and a finite second derivative with respect to z at $z = 0$. Thus, as expected, no surface divergence originates from this term. (The modifications introduced by renormalization are nonsingular at $z = 0$.)

On the other hand, the WKB expansion is effective for isolating the small-z behavior of the energy arising from g_{FF}. This expansion is valid for large κ, even for small z. The asymptotic behaviors of the Airy functions are [19]

$$\mathrm{Ai}(z) \sim \frac{1}{2\sqrt{\pi}} z^{-1/4} e^{-2z^{3/2}/3}(1 - c_1 z^{-3/2} + O(z^{-3})), \tag{B4a}$$

$$\mathrm{Bi}(z) \sim \frac{1}{\sqrt{\pi}} z^{-1/4} e^{2z^{3/2}/3}(1 + c_1 z^{-3/2} + O(z^{-3})) + O(e^{-2z^{3/2}/3}), \tag{B4b}$$

where $c_1 = 5/48$. Extrapolating to $z = 0$ (and dropping some κ-independent constants), these formulas suggest the initial data,

$$F(0) \sim \frac{1}{\sqrt{\kappa}} e^{-\Lambda(\kappa)}, \qquad F'(0) \sim -\sqrt{\kappa}\left(1 + \frac{v'(0)}{4\kappa^3}\right) e^{-\Lambda(\kappa)}, \tag{B5a}$$

$$G(0) \sim \frac{1}{\sqrt{\kappa}} e^{\Lambda(\kappa)}, \qquad G'(0) \sim \sqrt{\kappa}\left(1 - \frac{v'(0)}{4\kappa^3}\right) e^{\Lambda(\kappa)}, \tag{B5b}$$

where $\Lambda(\kappa) = \frac{2}{3}\kappa^{3/2}$. We have written Eqs. (B5) in a form that identifies them with the first-order WKB formulas (A3) and (A4a) for a particular choice of normalization, which makes the Wronskian independent of κ ($w = 2$, to be precise). This normalization can usefully be copied for dealing with other values of α. Note that $\Lambda \to \infty$ as $\kappa \to \infty$. Validity of Eq. (B5b) requires that κ be sufficiently large that both (a) the WKB approximation is accurate and (b) the recessive term in Eq. (B4b) is negligible. From Eqs. (B5), it follows that

$$\frac{G_-}{F_-} = \frac{\kappa\mathrm{Bi}(\kappa^2) - \mathrm{Bi}'(\kappa^2)}{\kappa\mathrm{Ai}(\kappa^2) - \mathrm{Ai}'(\kappa^2)} \sim \frac{1}{4\kappa^3} e^{4\kappa^3/3}, \tag{B6}$$

(c_1 having canceled), and hence

$$g_{FF} \sim -\frac{1}{16}\frac{v'(0)}{\kappa^4} e^{-2\kappa z}. \tag{B7}$$

The resulting term in u diverges at the boundary,

$$\alpha = 1\colon\ u_{\mathrm{surf}} = \frac{1 + 12\beta}{192\pi^2 z}, \tag{B8}$$

as reported in Eq. (6.7) and numerically validated in Fig. 2. (This calculation extrapolates the integrand (B7) down to $\kappa = 0$. In principle, we know how to improve it by the method of Ref. [11].)

It is now incumbent upon us to investigate in what way this result is dependent upon the "handbook" basis choice, $\{\mathrm{Ai}, \mathrm{Bi}\}$. As we have stressed repeatedly (Refs. [10,11], and the body of this paper), the Green's function must not change under rescalings $F \to mF$, $G \to nG$, nor under a replacement $G \to G + pF$, where m, n, and p may depend on κ. The rescalings are trivially taken care of by the Wronskian factors w in Eq. (B2), so long as one has resisted the temptation to replace w by its value in some particular basis. The p replacement is more subtle, however; although g of course remains unchanged, its division into the two terms of Eq. (B2) does not. In particular, one might choose G so that G_- is identically 0. (This is the case for the solution called H in Ref. [11].) Then $g_{FF} = 0$, and u must come entirely from g_{FG}. Thus, our attribution of the surface energy to the second term of the Green's function cannot be valid in complete generality. What is going on here? Let us return to Eq. (B6) and consider replacing Bi by $\mathrm{Bi} + p\mathrm{Ai}$. One sees that any admixture of Ai will give an exponentially subdominant contribution, unless $p(\kappa)$ contains a correspondingly large exponential factor. This suggests that our calculation captures the truth for any "natural" basis choice, one not involving such an exponential fine-tuning. One can easily see that the preferred solution called G in Ref. [11] (characterized by $G(0) = 0$) is proportional to $\mathrm{Bi} + p\mathrm{Ai}$ with $p = -2e^{4\kappa^3/3}(1 + 2c_1\kappa^{-3} + \cdots)$. For H, the other preferred solution in Ref. [11], the calculation is more complicated, but again p will equal $e^{4\kappa^3/3}$ times a weakly (algebraically) varying function of κ. Such basis solutions, however natural for our problem, must be regarded as rare.

Note that a small admixture of Ai will not change the initial data (B5b) significantly. In fact, there is no reason to expect that Bi satisfies Eq. (B5b) or any higher-order improvement of it exactly [equivalently, that the recessive term in (B4b) is exactly zero]. It is, therefore, legitimate to challenge the numerical verification that g_{FG} yields no surface divergence at all; more likely, one is present but

with such a tiny coefficient that it did not show up in the finite-precision numerical investigation.

Can these considerations be carried over to larger α? Since then $v'(0) = 0$, Eqs. (B5) lead to trivial results and must be replaced by higher-order approximations. For the quadratic wall, we go out to third WKB order [in the sense of Appendix A—that is, keeping q_2 in both the exponent and the prefactor of Eq. (A3)] and obtain from Eqs. (A3)–(A4b)

$$\begin{aligned} F(0) &\sim \left(\kappa + \frac{1}{4\kappa^3}\right)^{-1/2} e^{-\Lambda(\kappa)}, \\ F'(0) &\sim -\left(\kappa + \frac{1}{4\kappa^3}\right)^{1/2} e^{-\Lambda(\kappa)}, \end{aligned} \tag{B9a}$$

$$\begin{aligned} G(0) &\sim \left(\kappa + \frac{1}{4\kappa^3}\right)^{-1/2} e^{\Lambda(\kappa)}, \\ G'(0) &\sim \left(\kappa + \frac{1}{4\kappa^3}\right)^{1/2} e^{\Lambda(\kappa)}. \end{aligned} \tag{B9b}$$

Here Eq. (B9a) is ineluctable, but Eq. (B9b) incorporates the tacit assumption that G is a "natural" basis solution without a large recessive component, so that the surface divergence will come entirely from g_{FF}. [If the recessive term in G is significant at large κ, then (a) it may make a surface-divergent contribution to the g_{FG} term and (b) it may cause a compensating change in the g_{FF} term through the factor G_-. These two effects must cancel when the two terms are known exactly, since the full answer must be independent of the basis choice.] Now for large κ

$$\begin{aligned} F(0) - \frac{1}{\kappa}F'(0) &\sim \frac{2}{\sqrt{\kappa}} e^{-\Lambda(\kappa)}, \\ G(0) - \frac{1}{\kappa}G'(0) &\sim -\frac{1}{4}\frac{1}{\kappa^{9/2}} e^{\Lambda(\kappa)}, \end{aligned} \tag{B10}$$

and hence

$$g_{FF} \sim \frac{1}{16}\frac{1}{\kappa^5} e^{-2\kappa z}. \tag{B11}$$

In this case, the resulting integral for u diverges at the lower limit, $\kappa = 0$, so as in Ref. [10] it must be cut off at, say, $\kappa = 1$, yielding

$$\alpha = 2\colon\ u_{\text{surf}} = -\frac{1 + 12\beta}{96\pi^2}\Gamma(0, 2z). \tag{B12}$$

The ambiguity in this infrared cutoff (which would not be necessary at all in a more accurate treatment of small κ [11]) can be absorbed into the logarithmic ambiguity μ from the (ultraviolet) renormalization. As reported in Sec. VII, after this one undetermined constant is fixed, Eq. (B12) agrees with the numerics. [The leading asymptotic correction to g_{FF} for $\alpha = 2$ was used to approximate the integral from K to ∞ in Eqs. (7.7) and (7.10), so that part of the numerical agreement was foreordained. However, that part of the integral is only a small part of the total, and the numerical confirmation of Eq. (7.13) is nontrivial.]

Furthermore, both Eq. (B8) and Eq. (B12) match the calculations in Ref. [10] for the exterior region, strengthening our confidence that the nonrigorous argument in this appendix reflects reality. More precisely, result (B12) is exactly the negative of the density found on the other side of the wall in Ref. [10], with $z \to |z|$, while result (B8) is the same as in Ref. [10], including the sign.

The argument shows that there is no surface divergence for T_{zz}, because in a term proportional to $e^{-2\kappa z}$, in the construction (2.13d) the leading powers of κ cancel and leave a positive power of z:

$$T_{zz} \sim -z^{\alpha} I[g_{F^2}]. \tag{B13}$$

[1] H. B. G. Casimir, On the attraction between two perfectly conducting plates, Kon. Ned. Akad. Wetensch. Proc. **51**, 793 (1948).

[2] E. M. Lifshitz, The theory of molecular attractive forces between solids, Sov. Phys. JETP **2**, 73 (1956).

[3] I. D. Dzyaloshinskii, E. M. Lifshitz, and L. P. Pitaevskii, General theory of van der Waals forces, Usp. Fiz. Nauk **73**, 381 (1961) [Sov. Phys. Usp. **4**, 153 (1961)].

[4] C. Xiong, T. W. Kelsey, S. A. Linton, and U. Leonhardt, Casimir forces for inhomogeneous planar media, J. Phys. Conf. Ser. **410**, 012165 (2013).

[5] U. Leonhardt and W. M. R. Simpson, Exact solution for the Casimir stress in a spherically symmetric medium, Phys. Rev. D **84**, 081701 (2011).

[6] N. Graham, M. Quandt, and H. Weigel, Attractive electromagnetic Casimir stress on a spherical dielectric shell, Phys. Lett. B **726**, 846 (2013).

[7] M. Beauregard, M. Bordag, and K. Kirsten, Casimir energies in spherically symmetric background potentials revisited, J. Phys. A **48**, 095401 (2015).

[8] *Casimir Physics*, Lecture Notes in Physics No. 834, edited by D. Dalvit *et al.* (Springer, New York, 2011).

[9] J. D. Bouas, S. A. Fulling, F. D. Mera, K. Thapa, C. S. Trendafilova, and J. Wagner, Investigating the spectral geometry of a soft wall, *Spectral Geometry*, edited by A. H. Barnett *et al.*, *Proc. Symp. Pure Math.* 84, 139 (2012).
[10] K. A. Milton, Hard and soft walls, Phys. Rev. D **84**, 065028 (2011).
[11] S. W. Murray, C. M. Whisler, S. A. Fulling, J. Wagner, H. B. Carter, D. Lujan, F. D. Mera, T. E. Settlemyre, Vacuum energy density and pressure near a soft wall, arXiv:1512.09121.
[12] F. D. Mazzitelli, J. P. Nery, and A. Satz, Boundary divergences in vacuum self-energies and quantum field theory in curved spacetime, Phys. Rev. D **84**, 125008 (2011).
[13] S. A. Fulling, K. A. Milton, and J. Wagner, Energy density and pressure in power-wall models, Int. J. Mod. Phys. A **27**, 1260009 (2012); Int. J. Mod. Phys. Conf. Ser. **14**, 115 (2012).
[14] M. J. Duff, Twenty years of the Weyl anomaly, Classical Quantum Gravity **11**, 1387 (1994).
[15] R. M. Wald, Trace anomaly of a conformally invariant quantum field theory in curved spacetime, Phys. Rev. D **17**, 1477 (1978).
[16] S. M. Christensen, Vacuum expectation value of the stress tensor in an arbitrary curved background: The covariant point separation method, Phys. Rev. D **14**, 2490 (1976).
[17] T. S. Bunch, Calculation of the renormalized quantum stress tensor by adiabatic regularization in two-dimensional and four-dimensional Robertson-Walker space-times, J. Phys. A **11**, 603 (1978).
[18] S. L. Adler, J. Lieberman, and Y. J. Ng, Regularization of the stress-energy tensor for vector and scalar particles propagating in a general background metric, Ann. Phys. (N.Y.) **106**, 279 (1977).
[19] C. M. Bender and S. A. Orszag, *Advanced Mathematical Methods for Scientists and Engineers* (Springer, New York, 1999).
[20] S. L. Adler and J. Lieberman, Trace anomaly of the stress-energy tensor for massive vector particles propagating in a general background metric, Ann. Phys. (N.Y.) **113**, 294 (1978).
[21] R. M. Wald, The back reaction effect in particle creation in curved spacetime, Commun. Math. Phys. **54**, 1 (1977).
[22] S. M. Christensen, Regularization, renormalization and covariant geodesic point separation, Phys. Rev. D **17**, 946 (1978).
[23] V. Moretti, One loop stress tensor renormalization in curved background: The relation between zeta function and point splitting approaches, and an improved point splitting procedure, J. Math. Phys. **40**, 3843 (1999).
[24] P. B. Gilkey, *Invariance Theory, the Heat Equation, and the Atiyah–Singer Index Theorem* (Publish or Perish, Wilmington, DE, 1984).
[25] S. A. Fulling, *Aspects of Quantum Field Theory in Curved Space-Time* (Cambridge University Press, Cambridge, England, 1989).
[26] K. A. Milton, J. Wagner, and K. Kirsten, Casimir effect for a semitransparent wedge and an annular piston, Phys. Rev. D **80**, 125028 (2009).
[27] N. Fröman, Outline of a general theory for higher order approximations of the JWKB-type, Arkiv för Fysik **32**, 541 (1966).